

## Structural studies of oligonucleotides containing G-quadruplex motifs using AFM

L.T. Costa,<sup>a,b,c</sup> M. Kerkmann,<sup>d</sup> G. Hartmann,<sup>d</sup> S. Endres,<sup>d</sup> P.M. Bisch,<sup>b</sup>  
W.M. Heckl,<sup>a</sup> and S. Thalhammer<sup>a,\*</sup>

<sup>a</sup> Department of Geo- and Environment Sciences, LMU, Munich 80333, Germany

<sup>b</sup> Instituto de Biofísica Carlos Chagas Filho, UFRJ, Rio de Janeiro 21949-900, Brazil

<sup>c</sup> Centro de Biotecnologia, UFRGS, Porto Alegre 91501-970, Brazil

<sup>d</sup> Department of Internal Medicine, Division of Clinical Pharmacology, LMU, Munich 80333, Germany

Received 9 December 2003

### Abstract

G-quadruplex DNAs are cyclic arrays of four guanine bases binding by Hoogsteen hydrogen bonds, found in the telomeric regions of chromosomes and in transcriptional regulatory regions of several important oncogenes. Here, we used high resolution atomic force microscopy (AFM) to observe a specific guanine (G) tetrad mediated complex formation of oligonucleotides containing a G-quadruplex motifs (G-ODN) combined with a palindromic sequence under physiological extracellular conditions. These oligonucleotides have been investigated in correlation to their immunostimulatory effects. We observed structural dependence on ion concentration and G-ODN concentration, where high concentration self-assembled DNA networks were formed.

© 2003 Elsevier Inc. All rights reserved.

**Keywords:** AFM; Palindromic sequence oligonucleotides; G-wire; Self-assembled DNA network; Nanowire

DNA is a duplex molecule where two self-complementary strands are held together by Watson–Crick base pairing. Besides, DNA G (guanine)-rich sequences can form arrays of four hydrogen bonds in which each base acts as both donor and acceptor of two hydrogen bonds with other guanines, and the pairing between bases is of the Hoogsteen type [1]. These so-called G-quadruplex structures are found in the telomeric region of chromosomes, immunoglobulin switch regions, gene promoter regions, and sequences associated with human diseases (for recent reviews, see [2,3] and references cited therein). As telomere maintenance mechanisms and the transcriptional regulation of oncogene expression are of potential importance for drug design, G-quadruplexes have been proven to be potentially important targets in drug development [2].

A variety of G-quadruplex structures exist *in vitro* and can be classified in terms of their molecularity and strand orientation. DNA sequences which contain one G-rich repeat can associate into parallel G-quadruplexes [4]. DNA sequences containing two or more G-rich repeats have been shown to form G–G hairpins, which in turn dimerize to form either several types of stable biomolecular quadruplexes [5], or parallel [6] and anti-parallel [7] G-quadruplexes. Additionally, short G-rich oligonucleotides (G-ODN) with at least three consecutive guanine molecules can form stable G-quadruplex DNA structures in the presence of specific monovalent ( $\text{Na}^+$ ,  $\text{K}^+$ , and  $\text{Rb}^+$ ) and divalent metal cations ( $\text{Mg}^{2+}$ ,  $\text{Ca}^{2+}$ ,  $\text{Ba}^{2+}$ , and  $\text{Sr}^{2+}$ ) [8].

Microbial DNA is recognized by the human immune system based on the presence of unmethylated CG-dinucleotides, which in a certain base context are termed CpG-motifs. Synthetic oligonucleotides (ODN) containing this CpG-motif mimic microbial DNA and have shown immunostimulatory properties [9,10]. The Toll-like receptor 9 (TLR9) recognizes CpG-motifs [11].

\* Corresponding author. Fax: +49-8021-80-4331.

E-mail address: [s.thalhammer@lrz.uni-muenchen.de](mailto:s.thalhammer@lrz.uni-muenchen.de) (S. Thalhammer).

As TLR-9 is expressed on B-cells and plasmacytoid dendritic cells (PDC), these two cell-types are strongly activated by ODN containing CpG-motifs [12–14]. Their potent immunostimulatory effect makes them a promising candidate as an adjuvant treatment, not only in vaccine protocols but also in immunotherapy of cancer [10]. Recently, two different groups of these ODN have been defined due to their distinct immunostimulatory properties. G-ODN A (5'-ggG GGA CGA TCG TCg ggg gG-3') is characterized by a high induction of type I interferon (IFN) in PDC and strong natural killer cell activation, whereas ODN B (5'-tcg tcg ttt tgt cgt ttt gtc gtt-3') promotes stronger activation, survival, and maturation of PDCs, and B-cells than G-ODN A [15,16]. G-ODN A and ODN B also differ in their primary structure. The sequence of G-ODN A is characterized by two G-rich repeats and a central palindrome. In contrast, ODN B does not share any of these characteristics. Besides, G-ODN is able to self-organize a uniform two-dimensional reticulated self-assembled network formation and can act as a semiconducting nanowire [17–19].

High resolution atomic force microscopy (AFM) [20] has been used as a powerful tool for imaging DNA and DNA–protein structures [21,22]. So far, G-quadruplex structures have been studied by AFM [6,7], where the metal cation's influence on the structure was observed. Here, we present G-quadruplex AFM topographic data to comprehend whether the differential immunostimulatory properties of the G-ODN A and ODN B are correlated with their structural differences. Additionally, we show the dependence of the G-ODN A structure on ion concentration and on oligonucleotide concentration.

## Materials and methods

**Oligonucleotides.** The oligonucleotides used in this study were provided by Coley Pharmaceutical Group (Wellesley, MA, USA) and Metabion (Martinsried, Germany): G-ODN A (5'-ggG GGA CGA TCG TCg ggg gG-3'); ODN B (5'-tcg tcg ttt tgt cgt ttt gtc gtt-3'); and G-ODN Am (ggG GGT CGA ACG TCg ggg gG). Small letters describe phosphorothioate linkage, capital letters phosphodiester linkage 3' of the base, and bold CpG-dinucleotides.

**Sample preparation.** The oligonucleotides, diluted in Dulbecco PBS without Ca<sup>2+</sup> and Mg<sup>2+</sup> (ion concentration: 4.2 mM K<sup>+</sup>, 139 mM Na<sup>+</sup>) (Biochrom KG, Berlin, Germany), were deposited over pre-treated mica (25 mM MgCl<sub>2</sub>; spin coating by 1 min). To increase the DNA–mica binding in water experiments, the mica was pre-incubated with 20 µl of 100 mM MgCl<sub>2</sub> for 2 min, washed with ddH<sub>2</sub>O, and dried with a gentle N<sub>2</sub> flow. For samples diluted in G-buffer (50 mM KCl, 10 mM MgCl<sub>2</sub>, and 50 mM Tris–HCl (pH 7.0)), 5 µl was deposited on freshly cleaved mica, incubated for 5 min, washed with ddH<sub>2</sub>O, and dried under vacuum.

**AFM Microscopy.** For AFM microscopy a Topometrix Explorer (Darmstadt, Germany) was used, operating in dynamic mode under ambient conditions, with 40% relative humidity, using NSC11 cantilevers (Mikromasch, Estonia) with a spring constant of 3 N/m and a resonance frequency of ~45 kHz. The nominal tip radius was <10.0 nm. Image analysis was performed using SPIP software (Lynx, Denmark).

## Results and discussion

### AFM imaging of oligonucleotides

We used mica pre-treated with Mg<sup>2+</sup> to increase the binding between DNA and mica. Stable AFM image conditions make it possible to visualize specific oligonucleotide structures under several conditions, as physiological extracellular conditions (PBS), using high ionic concentration (G-buffer), and ddH<sub>2</sub>O. The binding stability was conferred by cation Mg<sup>2+</sup> over mica surface. In all images the sample conformation was preferentially flat due to ODN preparation based on a single drop spread over on the mica substrate.

### Structural correlation between G-ODN A and ODN B

First experiments were carried out to observe specific ODN structures diluted in physiological buffer (PBS) to correlate G-ODN A (Fig. 1A) and ODN B (Fig. 2) with their biological function. Fig. 1A shows a heterogeneous distribution of G-ODN A structures. Predominantly were observed globular structures with a media in height of (3.8 ± 0.7) nm and diameter of (46.2 ± 3.9) nm. The histograms of diameter and height distribution are shown in Figs. 1B and C, respectively. Besides these globular structures were also detected interconnected structures with lengths from 80 to >130 nm, height in a range of 1.8–10 nm, and diameter of 2.0–30 nm. The average data were taken from several different experiments. Such heterogeneous structure formations were also detected by gel electrophoresis assays (Kerkmann et al., in preparation). By analyzing ODN B images, no three-dimensional structure formation was observed. In contrast, only by cross section height analysis it was possible to observe a layer over the mica surface with an average height of around 1.2 nm (Fig. 2).

G-ODN A and ODN B differ in their immunostimulatory properties. G-ODN A induces very high amounts of type I IFN in PDC. However, G-ODN A is a poor inducer of activation markers in PDCs and does not activate B-cells at all. In contrast, ODN B is a very strong B-cell-mitogen and a strong activator of activation markers in PDCs. However, induction of type I IFN in PDCs by ODN B is quite low. Therefore, it was investigated whether the differential immunostimulatory properties of G-ODN A and ODN B might be correlated with structural differences. For this, both structures were analyzed under therapeutical conditions to distinguish between the two ODNs in their ability to form specific structures. The G-ODN A sequence is characterized by two G-rich repeats and a central palindrome, which allows the establishment of Watson–Crick hydrogen bonding. By this, it can form hairpin dimers, parallel tetramers, and higher order structures, as interconnected structures. The G-ODN A

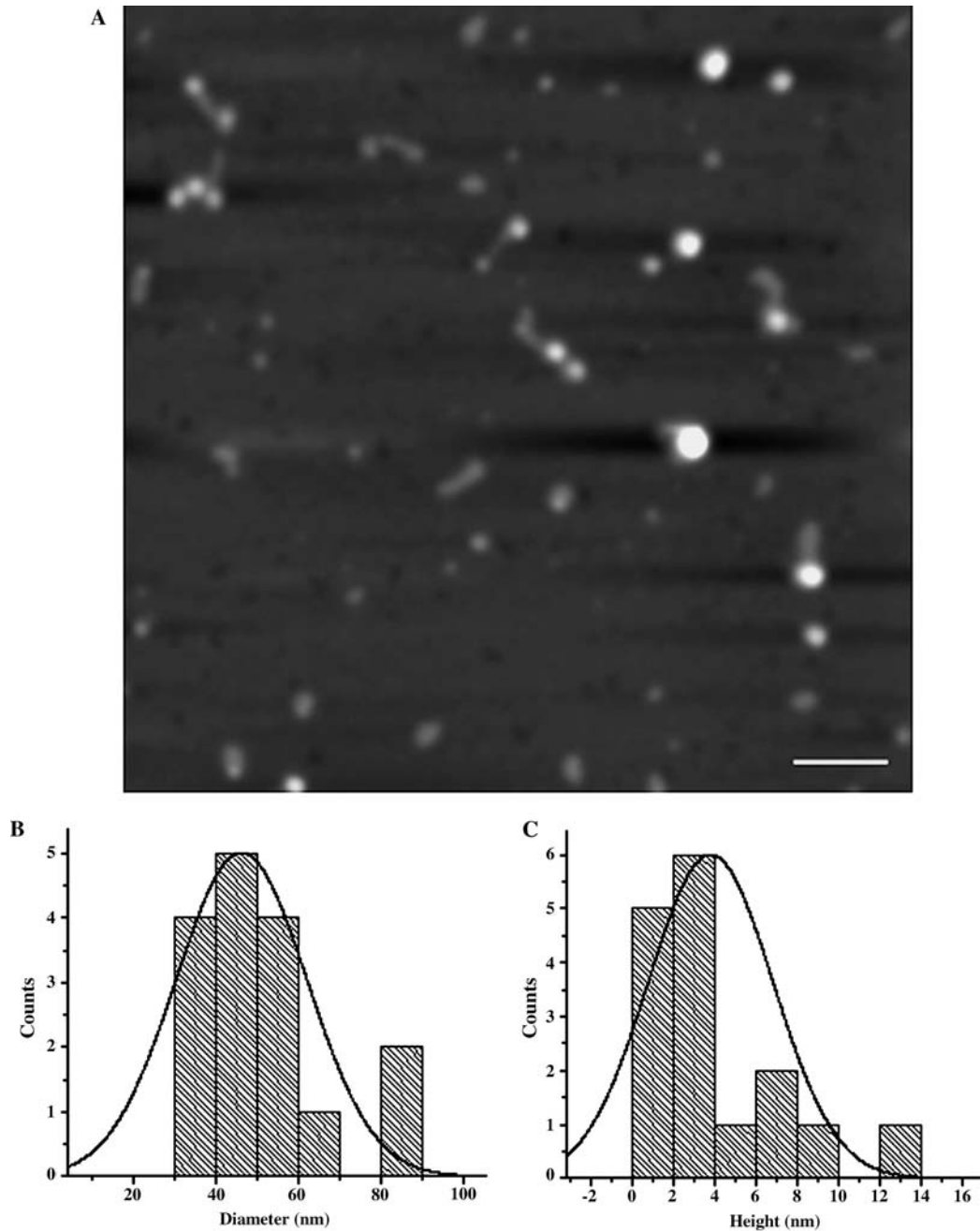


Fig. 1. (A) Dynamic-mode AFM image taken in air of G-ODN A on  $Mg^{2+}$  pre-treated mica. G-ODN A diluted in PBS at  $6 \mu\text{g/ml}$ . Scale bar is 100 nm. The histograms from the globular structures show the following distribution in diameter (B) and height (C).

concentration and cationic environment determine the predominate conformations. G-ODN A structure (Fig. 1A) under therapeutical conditions reveals a heterogeneous formation. Concerning the possible equilibrium arrangements between G-quadruplex and Watson–Crick bonding formation, the structure formation based on the aggregation of single strands is hypothesized. Such hypothesis has also been supported by recent data in the literature, where it was demonstrated that similar G-ODN diluted in PBS form an extremely heterogeneous mixture of secondary struc-

tures with very high-order aggregates containing more than 30 G-ODN strands [23]. In contrast, ODN B does not share the same sequence characteristics as G-ODN A. In this case, the presented AFM data (Fig. 2) revealed neither globular structures nor interconnections over the mica surface, clearly due to the ODN B sequence features, where no G-quadruplexes binding or single Watson–Crick bond can be formed. Combining the described immunostimulatory effect with our AFM data, the globular structure as well as interconnected structure formation of G-ODN A may play a role in the

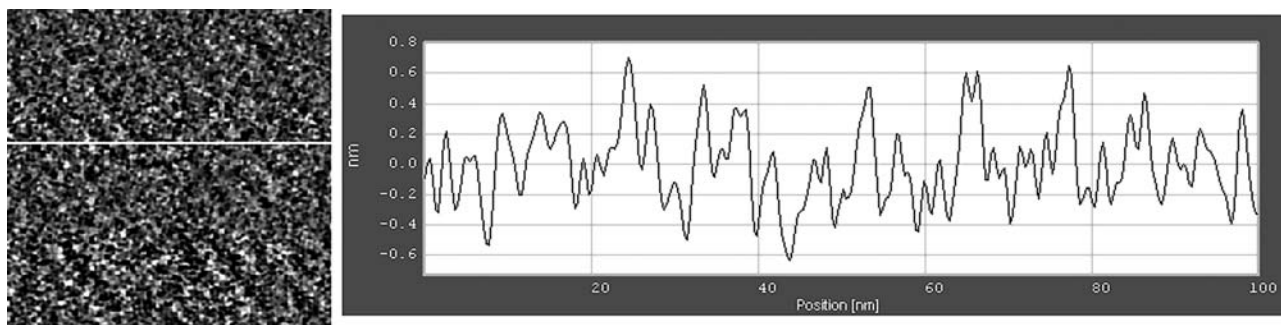


Fig. 2. ODN B diluted in PBS at  $6\mu\text{g/ml}$  on  $\text{Mg}^{2+}$  pre-treated mica. Cross section analysis shows the average height of 1.2 nm. The image was acquired using dynamic mode in air. Scan size is 100 nm.

therapeutical applications in contrast with ODN B that does not form any particular structure. Additionally, in vivo effects of G-ODN A and ODN B have been recently shown by means of biochemistry and immunoassays (Kerkmann et al., in preparation).

#### *Palindromic sequence effect*

Using a modified G-ODN A without palindromic sequence (G-ODN Am), under the same conditions, it was possible to observe homogeneous structures with different dimensions (Fig. 3A). Analyzing the histogram distribution, G-ODN Am structures present an average diameter of  $(53.5 \pm 2.8)\text{nm}$  (Fig. 3B) and height of  $(1.64 \pm 0.15)\text{nm}$  (Fig. 3C). These data compared to those presented for G-ODN A suggested that interconnected structure formation was due to the presence of a palindromic sequence. Also, in G-ODN Am images we could observe a height compressibility effect due to the cationic conditions. Recent AFM experiments with oligonucleotides containing only G-rich sequence have revealed aggregates of a kind of sphere with about 41.67 nm in diameter and 1.65 nm in height [24].

G-quadruplex aggregates formed by double G-rich repeats tend to assemble into dimeric structures by the association of hairpin pairs. Several structures of double G-rich repeats have been depicted by X-ray and NMR, and the extreme polymorphism of this family of quadruplexes illustrates the dependence of the quadruplex structure on the nucleotide content and sequence [3]. Single tracts of guanine associates mostly form parallel four-stranded structures. Folded structures are kinetically favored, but higher molecularity structures are favored at high DNA concentrations or conditions that disfavor loop formation such as high ion concentrations. Furthermore, the presence of potential Watson–Crick base pairs within a G-rich sequence has a profound effect on the final structure of a folded quadruplex due to the initial folding of the strand by formation of Watson–Crick base pairs [25]. Here, we observed the total absence of interconnected structure in the G-ODN A without palindromic sequence. It remains that only the

globular structures are smaller in height than those showed by G-ODNA. The immunostimulatory effect of that structure is still unknown.

#### *G-ODN A structure: buffer dependence*

To analyze the ion effect on G-ODN A structure, image acquisition was performed using G-ODN A diluted in G-buffer (Fig. 4A) (see Materials and methods) and distilled water (Fig. 4D). G-buffer consists of a high ionic concentration in comparison to PBS. Under this condition G-ODN A presented globular structures with a diameter of  $(38.3 \pm 5.4)\text{nm}$  (Fig. 4B) and a height of  $(2.1 \pm 0.3)\text{nm}$  (Fig. 4C). Also a few interconnected structures range in length from 100 to 160 nm, height from 2.0 to 2.8 nm, and in diameter from 2.0 to 2.8 nm. Moreover, G-ODN A diluted in ddH<sub>2</sub>O revealed globular structures with very high diameter  $(78.3 \pm 6.3)\text{nm}$  (Fig. 4E) and height  $(21.2 \pm 1.2)\text{nm}$  (Fig. 4F). G-rich DNA can form pre-G-quadruplex structures under physiological  $\text{Na}^+$  and  $\text{K}^+$  concentrations in vitro. The structures and stabilities of quadruplex DNAs are known to be dependent on the nature and concentrations of monovalent cations present in the solution. Monovalent cations ( $\text{K}^+$  and  $\text{Na}^+$ ) greatly stabilize G-quadruplex structures, presumably by coordinating with eight carbonyl oxygen atoms present between stacked tetrads [26]. Divalent ions also interact with DNA–quadruplex structures [27]. The primary formation of G-quadruplexes requires the presence of metal cations [3], as divalent cations to play an essential role in the G-quadruplex stabilization [28,29]. The balance between the kinetics of structure formation and the stability of a structure is an important factor in determining the favored conformation [30]. The coordination sites along the central axis of G-quadruplexes are not the only binding sites for metal ions. There are weak binding sites for divalent cations in the narrow grooves of dimeric hairpin quadruplexes and intramolecularly folded quadruplexes [28]. Data from AFM shown that only relatively short G-quadruplexes (so-called G-wires) were generated in the presence of  $\text{Na}^+$  or  $\text{K}^+$ .

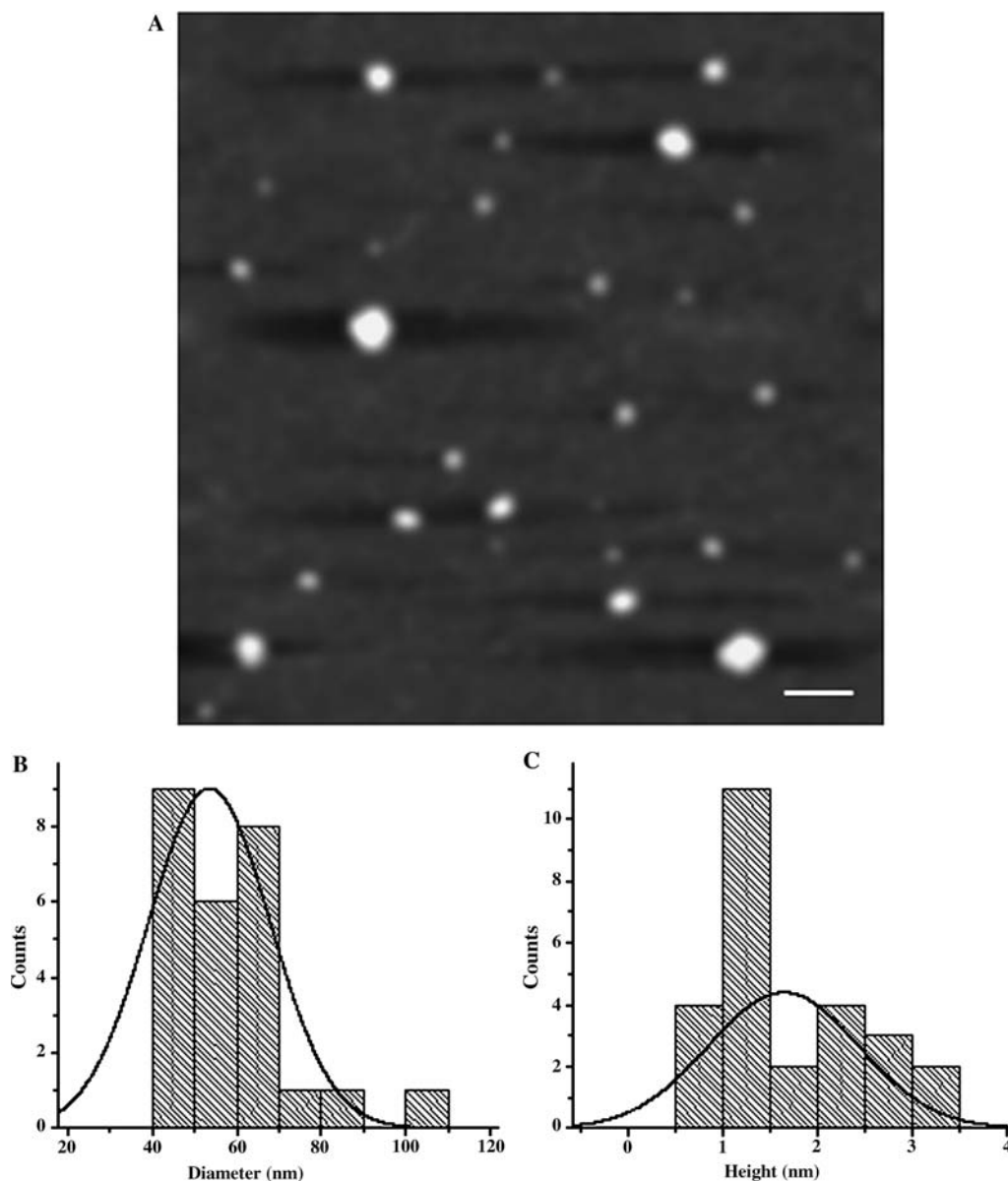


Fig. 3. (A) Dynamic-mode AFM image of G-ODN Am (G-ODN A without central palindromic sequence) diluted in PBS at 6  $\mu\text{g/ml}$ . Scale bar is 100 nm. The histograms show the distribution in diameter (B) and height (C).

With  $\text{Mg}^{2+}$ , longer G-wires were observed at low frequency [6]. The height of G-wire depends on the growth conditions and moreover G-wire compressibility is a function of cationic growth conditions. Furthermore, it was reported that the presence of  $\text{Mg}^{2+}$  in growing conditions greatly facilitates the aggregate formation [1]. The coordinating cation provides additional stability to the structure, thereby providing resistance to a conformation change upon surface binding [6]. Comparing our AFM data (Figs. 1A and 4A), it becomes clear about the correlation between G-ODN A structure and the ion concentration. Although G-ODN A structures diluted in G-buffer are comparable in length to those obtained with G-ODN A in PBS (Fig. 1A), the height was not higher than 2.8 nm, which suggests a predominant

G-wire formation instead of interconnected structures. Furthermore, G-ODN A dissolved in distilled water revealed huge globular structures that may represent aggregates of several single and/or double stranded oligonucleotides. Such an effect is simply explained by the DNA hydrophobic features in  $\text{ddH}_2\text{O}$ , without any particular structure correlation with the ODN sequence content. Those data indicate a central role of G-ODN A interconnected structure formation in the immunostimulatory effect.

#### *G-ODN A structure: concentration dependence*

All previous images were taken using the therapeutic concentration of G-ODN A (6  $\mu\text{g/ml}$ ). To study G-ODN

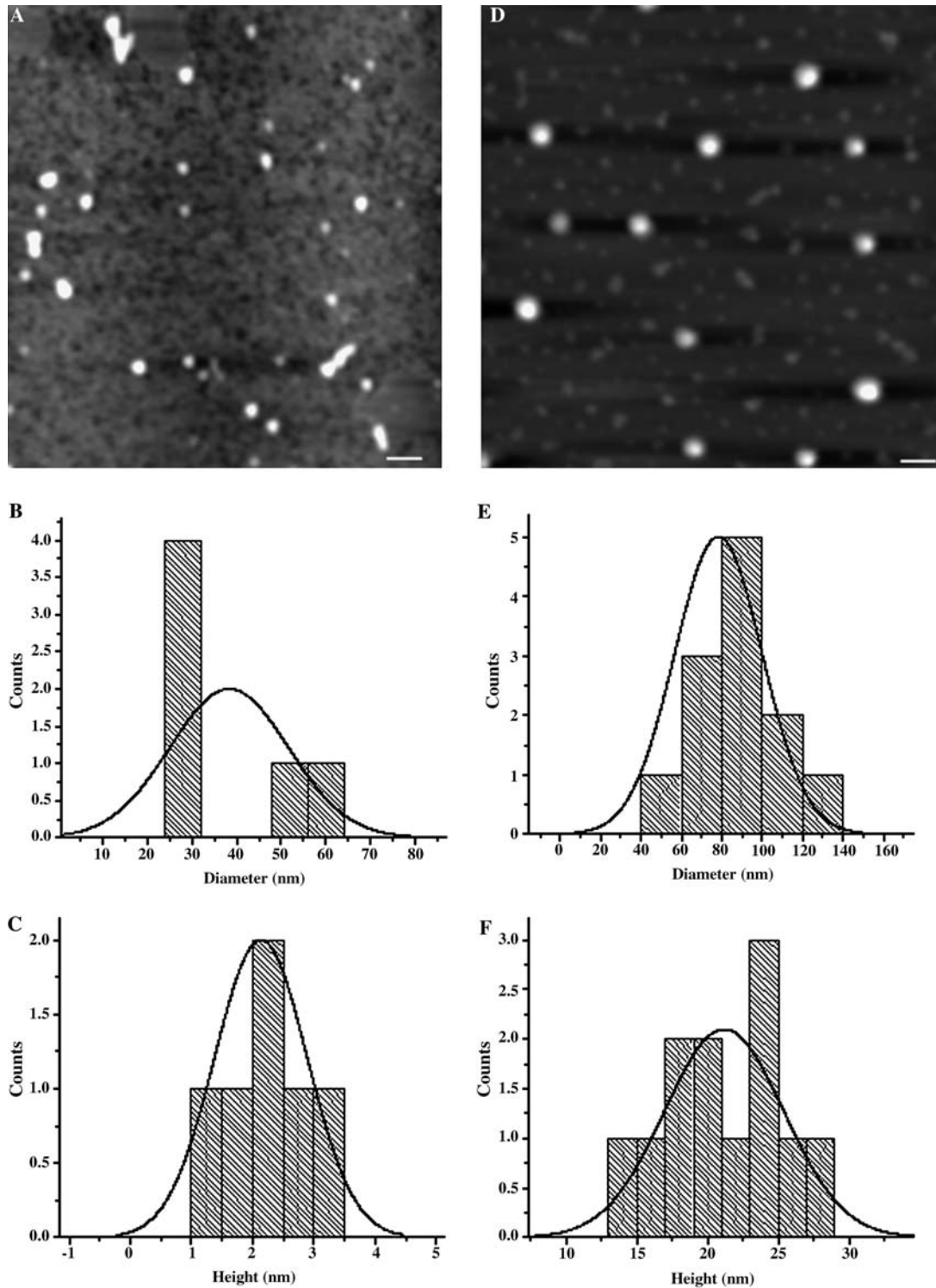


Fig. 4. Dynamic-mode AFM image of G-ODN A (6  $\mu\text{g/ml}$ ) diluted in (A) G-buffer (see Materials and methods) and (D) diluted in ddH<sub>2</sub>O. Scale bar is 100 nm. The histograms show a distribution in diameter (C) and height (D) of G-ODN A diluted in G-buffer, and diameter (E) and height (F) of G-ODN A diluted in ddH<sub>2</sub>O.

A structure concentration dependence, images were acquired using G-ODN A at 125  $\mu\text{g/ml}$  (Fig. 5). It was possible to observe G-ODN A self-assembly, forming a complex network structure. G-ODN A network

revealed a homogeneous height of around 2–3 nm (cross section analysis), predominantly as an infinite tetramer connection. Such AFM data show that under high G-ODN A concentration no specific structure is formed,

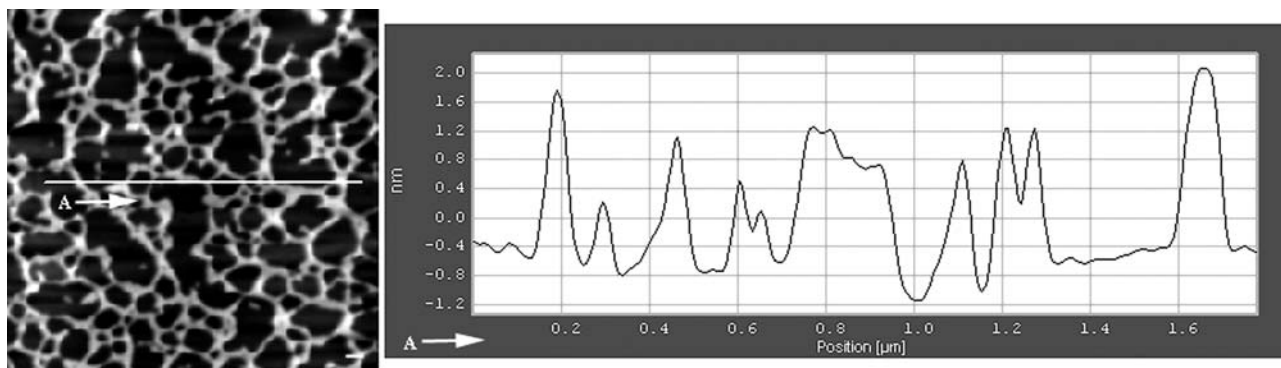


Fig. 5. Representative AFM image of G-ODN A self-assembled on freshly cleaved mica. G-ODN A was diluted in G-buffer at higher concentration (125  $\mu\text{g}/\text{ml}$ ) than used in therapeutical conditions. The cross section analysis (in the direction of A) reveals the average height of G-ODN A network. Scale bar is 100 nm.

just a DNA network can be observed. DNA network has been largely studied due its possible use as a semiconductor device [17–19]. Previously, AFM G-quadruplex studies were carried out using high ODN concentration (250  $\mu\text{g}/\text{ml}$ ), the nanostructure showed length in the range from 10 to >1000 nm and height from 1.27 to 2.39 nm [6].

AFM topographic data have revealed G-quadruplex oligonucleotide (G-ODN) structure sequence's dependence under physiological conditions, as well as the structure's dependence on ion concentration and G-ODN concentration. Therefore, AFM has revealed as a powerful tool to investigate ODN-sequence dependent structures, and their correlation with immunostimulatory effects. In future, the challenge will be to correlate G-ODN structure with *in vivo* functions. Besides, G-ODN is a promising candidate as a component for nanowires and as a building block for directing the assembly of nanoscale components into higher ordered structures.

### Acknowledgment

The authors thank for the financial support provided by DAAD and DFG SFB 486/Germany.

### References

- [1] F. Sha, R. Mu, D. Henderson, F. Chen, Self-aggregation of DNA oligomers with XGG trinucleotide repeats: kinetic and atomic force microscopy measurements, *Biophys. J.* 77 (1999) 410–423.
- [2] H. Han, L.H. Hurley, G-quadruplex DNA: a potential target for anti-cancer drug design, *TIPS* 21 (2000) 136–142.
- [3] M.A. Keniry, Quadruplex structures in nucleic acids, *Biopolymers* 56 (2001) 123–146.
- [4] D. Sen, W. Gilbert, Formation of parallel four-stranded complexes by guanine-rich motifs in DNA and its implication for meiosis, *Nature* 334 (1988) 364–366.
- [5] C. Kang, X. Zhang, R. Ratliff, R. Moyzis, A. Rich, Crystal structure of four-stranded Oxytricha telomeric DNA, *Nature* 356 (1992) 126–131.
- [6] T.C. Marsh, J. Vesenska, E. Henderson, A new DNA nanostructure the G-wire, imaged by scanning probe microscopy, *Nucleic Acids Res.* 23 (1995) 696–700.
- [7] D. Miyoshi, A. Nakao, N. Sugimoto, Structural transition from antiparallel to parallel G-quadruplex of  $d(\text{G}_4\text{T}_4\text{G}_4)$  induced by  $\text{Ca}^{2+}$ , *Nucleic Acids Res.* 31 (2003) 1156–1163.
- [8] E.A. Venczel, D. Sen, Parallel and antiparallel G-DNA structures from a complex telomeric sequence, *Biochemistry* 32 (1993) 6220–6228.
- [9] A.M. Krieg, A.K. Yi, S. Matson, T.J. Waldschmidt, G.A. Bishop, R. Teasdale, G.A. Koretzky, D.M. Klinman, CpG motifs in bacterial DNA trigger direct B-cell activation, *Nature* 374 (1995) 546–549.
- [10] A.M. Krieg, CpG motifs in bacterial DNA and their immune effects, *Annu. Rev. Immunol.* 20 (2002) 709–760.
- [11] H. Hemmi, O. Takeuchi, T. Kawai, T. Kaisho, S. Sato, H. Sanjo, M. Matsumoto, K. Hoshino, H. Wagner, K. Takeda, S. Akira, A Toll-like receptor recognizes bacterial DNA, *Nature* 408 (2000) 740–745.
- [12] G. Hartmann, A.M. Krieg, Mechanism and function of a newly identified CpG DNA motif in human primary B cells, *J. Immunol.* 164 (2000) 944–953.
- [13] A. Krug, A. Towarowski, S. Britsch, S. Rothenfusser, V. Hornung, R. Bals, T. Giese, H. Engelmann, S. Endres, A.M. Krieg, G. Hartmann, Toll-like receptor expression reveals CpG DNA as a unique microbial stimulus for plasmacytoid dendritic cells which synergizes with CD40 ligand to induce high amounts of IL-12, *Eur. J. Immunol.* 31 (2001) 3026–3037.
- [14] V. Hornung, S. Rothenfusser, S. Britsch, A. Krug, B. Jahrsdorfer, T. Giese, S. Endres, G. Hartmann, Quantitative expression of Toll-like receptor 1–10 mRNA in cellular subsets of human peripheral blood mononuclear cells and sensitivity to CpG oligodeoxynucleotides, *J. Immunol.* 168 (2002) 4531–4537.
- [15] A. Krug, S. Rothenfusser, V. Hornung, B. Jahrsdorfer, S. Blackwell, Z.K. Ballas, S. Endres, A.M. Krieg, G. Hartmann, Identification of CpG oligonucleotides sequences with high induction of IFN- $\alpha/\beta$  in plasmacytoid dendritic cells, *Eur. J. Immunol.* 31 (2001) 2154–2163.
- [16] M. Kerkmann, S. Rothenfusser, V. Hornung, A. Towarowski, M. Wagner, A. Sarris, T. Giese, S. Endres, G. Hartmann, Activation with CpG-A and CpG-B oligonucleotides reveals two distinct regulatory pathways of Type I IFN synthesis in human plasmacytoid dendritic cells, *J. Immunol.* 170 (2003) 4465–4474.

- [17] L. Cai, H. Tabata, T. Kawai, Self-assembled DNA networks and their electrical conductivity, *Phys. Rev. Lett.* 77 (2000) 3105–3106.
- [18] T. Kanno, H. Tanaka, Formation and control of two-dimensional deoxyribonucleic acid network, *Appl. Phys. Lett.* 77 (2000) 3848–3850.
- [19] J. Gu, S. Tanaka, Y. Otsuka, H. Tabata, T. Kawai, Self-assembled dye-DNA network and its photoinduced electrical conductivity, *Appl. Phys. Lett.* 80 (2002) 688–690.
- [20] G. Binnig, C.F. Quate, Ch. Gerber, Atomic force microscope, *Phys. Rev. Lett.* 56 (1986) 930–933.
- [21] H. Hansma, J. Vesenka, C. Siegerist, G. Kelderman, H. Morrett, R.L. Sinsheimer, V. Elings, C. Bustamante, P.K. Hansma, Reproducible imaging and dissection of plasmid DNA under liquid with the atomic force microscope, *Science* 256 (1992) 1180–1184.
- [22] H.G. Hansma, D.E. Laney, M. Bezanilla, R.L. Sinsheimer, P.K. Hansma, Applications for atomic force microscopy of DNA, *Biophys. J.* 68 (1995) 1672–1677.
- [23] J.D. Marshall, K. Fearon, C. Abbate, S. Subramanian, P. Yee, J. Gregorio, R.L. Coffman, G.V. Nest, Identification of a novel CpG DNA class and motif that optimally stimulate B cell and plasmacytoid dendritic cell functions, *J. Leuk. Biol.* 73 (2003) 781–792.
- [24] C. Zhou, Z. Tan, C. Wang, Z. Wei, Z. Wang, C. Bai, J. Qin, E. Cao, Branched nanowire based guanine rich oligonucleotides, *J. Biomol. Struct. Dyn.* 18 (2001) 807–812.
- [25] P. Balagurumoorthy, S.K. Brahmachari, Structure and stability of human telomeric sequence, *J. Biol. Chem.* 269 (1994) 21858–21869.
- [26] J.R. Williamson, M.K. Raghuraman, T.R. Cech, Monovalent cation-induced structure telomeric DNA: the G-quartet model, *Cell* 59 (1989) 871–880.
- [27] V.M. Marathias, P.H. Bolton, Determinants of DNA quadruplex structural type: sequence and potassium binding, *Biochemistry* 38 (1999) 4355–4364.
- [28] V.M. Marathias, K.Y. Wang, S. Kumar, T.Q. Pham, S. Swaminathan, P.H. Bolton, Determination of the number and location of the manganese binding sites of DNA quadruplexes in solution by EPR and NMR in the presence and absence of thrombin, *J. Mol. Biol.* 260 (1996) 378–394.
- [29] N. Spackova, I. Berger, J. Sponer, Nanosecond molecular dynamics simulations of parallel and antiparallel guanine quadruplex DNA molecules, *J. Am. Chem. Soc.* 121 (1999) 5519–5534.
- [30] T.C. Marsh, E. Henderson, G-wires: self-assembly of a telomeric oligonucleotides, d(GGGGTTGGGG), into large structures, *Biochemistry* 33 (1994) 10718–10724.